



The *Arabidopsis* CERK1-associated kinase PBL27 connects chitin perception to MAPK activation

Kenta Yamada^{1,†}, Koji Yamaguchi^{1,†}, Tomomi Shirakawa¹, Hirofumi Nakagami^{2,‡}, Akira Mine^{3,4,‡}, Kazuya Ishikawa¹, Masayuki Fujiwara⁵, Mari Narusaka⁶, Yoshihiro Narusaka⁶, Kazuya Ichimura^{2,7}, Yuka Kobayashi¹, Hidenori Matsui², Yuko Nomura², Mika Nomoto⁴, Yasuomi Tada⁴, Yoichiro Fukao⁸, Tamo Fukamizo¹, Kenichi Tsuda³, Ken Shirasu², Naoto Shibuya⁹ & Tsutomu Kawasaki^{1,*}

Abstract

Perception of microbe-associated molecular patterns by host cell surface pattern recognition receptors (PRRs) triggers the intracellular activation of mitogen-activated protein kinase (MAPK) cascades. However, it is not known how PRRs transmit immune signals to MAPK cascades in plants. Here, we identify a complete phospho-signaling transduction pathway from PRR-mediated pathogen recognition to MAPK activation in plants. We found that the receptor-like cytoplasmic kinase PBL27 connects the chitin receptor complex CERK1-LYK5 and a MAPK cascade. PBL27 interacts with both CERK1 and the MAPK kinase kinase MAPKKK5 at the plasma membrane. Knockout mutants of *MAPKKK5* compromise chitin-induced MAPK activation and disease resistance to *Alternaria brassicicola*. PBL27 phosphorylates MAPKKK5 *in vitro*, which is enhanced by phosphorylation of PBL27 by CERK1. The chitin perception induces disassociation between PBL27 and MAPKKK5 *in vivo*. Furthermore, genetic evidence suggests that phosphorylation of MAPKKK5 by PBL27 is essential for chitin-induced MAPK activation in plants. These data indicate that PBL27 is the MAPKKK kinase that provides the missing link between the cell surface chitin receptor and the intracellular MAPK cascade in plants.

Keywords MAPKKK5; PAMP; plant immunity; RLCK; signal transduction

Subject Categories Microbiology, Virology & Host Pathogen Interaction; Plant Biology; Signal Transduction

DOI 10.15252/embj.201694248 | Received 3 March 2016 | Revised 26 August 2016 | Accepted 30 August 2016 | Published online 27 September 2016

The EMBO Journal (2016) 35: 2468–2483

Introduction

Plants have evolved a sophisticated immune system to detect and defend against potential pathogens. The immunity is initiated by the perception of highly conserved microbe-associated molecular patterns (MAMPs), including bacterial flagellin, peptidoglycan (PGN), and fungal chitin, which trigger a series of immune responses referred to as pattern-triggered immunity (PTI) (Dangl *et al.*, 2013). However, successful pathogens can dampen or suppress PTI by delivering effector proteins into the host cytoplasm (Dou & Zhou, 2012). To overcome this, plants have developed a second layer of immune system, in which intracellular immune receptors of the nucleotide-binding leucine-rich repeat (NB-LRR) protein family directly or indirectly recognize the effectors and activate immune responses that are often associated with hypersensitive cell death (Dodds & Rathjen, 2010). This type of immunity is termed effector-triggered immunity (ETI) (Jones & Dangl, 2006).

Microbe-associated molecular patterns are perceived by cell surface-localized pattern recognition receptors (PRRs). All well-characterized PRRs are receptor-like kinase (RLKs) or receptor-like proteins (RLPs) (Monaghan & Zipfel, 2012). Both types of PRRs contain a ligand-binding ectodomain and a transmembrane domain, but only RLKs have an intercellular kinase domain (Macho & Zipfel, 2014). The perception of ligands with PRRs triggers a series of immune responses including a rapid intracellular activation of mitogen-activated protein kinase (MAPK) cascades and a burst of reactive oxygen species (ROS) mediated by NADPH oxidase (Macho & Zipfel, 2014).

In eukaryotes, MAPK cascades consist of highly conserved signaling modules. Each MAPK cascade is composed of three

1 Department of Advanced Bioscience, Graduate School of Agriculture, Kindai University, Nakamachi, Nara, Japan

2 RIKEN Center for Sustainable Resource Science, Tsurumi-ku, Yokohama, Japan

3 Department of Plant Microbe Interactions, Max Planck Institute for Plant Breeding Research, Cologne, Germany

4 Center for Gene Research, Nagoya University, Chikusa-Ku, Nagoya, Japan

5 Institute for Advanced Biosciences, Keio University, Tsuruoka, Yamagata, Japan

6 Research Institute for Biological Sciences Okayama, Kaga-gun, Okayama, Japan

7 Faculty of Agriculture, Kagawa University, Miki-cho, Kita-gun, Kagawa, Japan

8 Department of Bioinformatics, Ritsumeikan University, Kusatsu, Shiga, Japan

9 Department of Life Sciences, School of Agriculture, Meiji University, Tama-ku, Kawasaki, Kanagawa, Japan

*Corresponding author. Tel: +81 742 43 7335; E-mail: t-kawasaki@nara.kindai.ac.jp

†These authors contributed equally to this work as first authors

‡These authors contributed equally to this work as third authors

consecutively acting protein kinases: a MAPK kinase kinase (MAPKKK; 80 genes in *Arabidopsis*), a MAPK kinase (MAPKK; 10 genes in *Arabidopsis*), and a MAPK (20 genes in *Arabidopsis*) (Jonak et al, 2002). Increasing evidence indicates the importance of MAPKs in plant immunity; the activation of MAPKs induces robust immune responses through the phosphorylation of transcription factors and enzymes (Asai et al, 2002; Tsuda et al, 2013; Lee et al, 2015). MAPKs also regulate growth and development in plants, which can also be activated by RLK-mediated perception of self-derived molecules including secreted peptides (Meng et al, 2015). Thus, PRR/RLK-mediated activation of MAPKs plays important roles in both plant immunity and development. However, the molecular mechanisms by which PRRs/RLKs transmit signals to the MAPK cascades have not been found.

Arabidopsis PRRs FLS2 and EFR are RLKs with extracellular leucine-rich repeat (LRR) domains for the perception of bacterial flagellin and elongation factor Tu (EF-Tu), respectively (Monaghan & Zipfel, 2012). The perception of ligands by FLS2 or EFR induces their association with the coreceptor RLK BAK1 (Chinchilla et al, 2007; Heese et al, 2007; Schwessinger et al, 2011; Sun et al, 2013). FLS2 and EFR also associate with the receptor-like cytoplasmic kinases (RLCKs) BIK1, PBL1, and BSK1 (Lu et al, 2010; Zhang et al, 2010; Shi et al, 2013), which are phosphorylated and released from the FLS2 and EFR complexes upon ligand perception. Recent investigations indicated that BIK1 directly regulates NADPH oxidase RBOHD activation by phosphorylation of the N-terminal regulatory domain of RBOHD (Kadota et al, 2014; Li et al, 2014). However, loss-of-function mutations of *BIK1*, *PBL1*, and *BSK1* do not affect FLS2/EFR-mediated MAPK activation (Feng et al, 2012; Shi et al, 2013; Ranf et al, 2014). Thus, it is currently unclear how MAPK cascades are activated downstream of FLS2 and EFR.

Four MAPKs, MPK3, MPK4, MPK6, and MPK11, have been investigated to be activated by PAMPs. Genetic and biochemical studies revealed two MAPK cascades (Rasmussen et al, 2012): MKK4/MKK5 (two redundant MAPKKs)–MPK3/MPK6 (two partially redundant MAPKs) and MEKK1 (MAPKKK)–MKK1/MKK2 (two redundant MAPKKs)–MPK4 (MAPK). Although transient expression of MEKK1 in protoplasts activates MPK3 and MPK6 (Asai et al, 2002), flg22-induced activation of MPK3 and MPK6 was not affected by the *mekk1* mutation (Suarez-Rodriguez et al, 2007). Thus, MAPKKKs upstream of MPK3 and MPK6 have not been genetically identified in FLS2-mediated signaling so far.

Chitin, a fungal-derived molecule, is recognized by CEBiP, a rice PRR with an extracellular lysine motif (LysM) domain (Kaku et al, 2006). The LysM domain of CEBiP binds directly to chitin and forms a receptor complex with LysM-RLK OsCERK1 (Shimizu et al, 2010; Hayafune et al, 2014). OsCERK1 phosphorylates OsRLCK185, and silencing of OsRLCK185 reduces chitin-induced MAPK activation (Yamaguchi et al, 2013), suggesting that OsRLCK185 functions downstream of OsCERK1 and upstream of the MAPK cascade. Recently, OsRLCK176, a rice homolog of BIK1, was also reported to participate in MAPK activation downstream of OsCERK1 (Ao et al, 2014). In *Arabidopsis*, the LysM-RLKs LYK5-CERK1 complex recognizes chitin (Liu et al, 2012; Cao et al, 2014), which induces CERK1-mediated phosphorylation of PBL27, the *Arabidopsis* homolog of OsRLCK185 (Shinya et al, 2014). The *pbl27* mutation reduces chitin-induced MAPK activation. These results suggested that OsRLCK185/OsRLCK176 and PBL27 may be functional links

between chitin receptors and the MAPK cascade in rice and *Arabidopsis*, respectively.

Here, we show that CERK1-associated kinase PBL27 interacts with MAPKKK5 at the plasma membrane. The *mapkkk5* mutations compromised chitin-induced MAPK activation. PBL27 phosphorylates MAPKKK5 in a CERK1-dependent manner. MAPKKK5 is disassociated from PBL27 in response to chitin. In addition, MAPKKK5 interacts with MKK4 and MKK5 *in vivo* and phosphorylates their activation loops. These results reveal a phospho-signaling pathway from CERK1-mediated pathogen recognition to the MAPK activation. Our study shows that PBL27 is the molecular element linking the cell surface chitin receptor and the intracellular MAPK cascade.

Results

MAPKKK5 regulates chitin-induced MAPK activation

CERK1 phosphorylates PBL27 in a ligand-dependent manner, and the *pbl27* mutation compromises chitin-induced MAPK activation (Shinya et al, 2014). These results raised the possibility that PBL27 directly transmits CERK1 activation to MAPKKKs, the starting molecules of the MAPK cascade. We carried out yeast two-hybrid assay to examine the interaction of PBL27 with 21 *Arabidopsis* MAPKKKs belonging to the MEKK subfamily (Fig EV1A) (Jonak et al, 2002), because some members of this subfamily have been reported to be involved in immunity (Rasmussen et al, 2012). PBL27 interacted strongly with MAPKKK5 (At5g66850) and weakly with MAPKKK3 (At1g53570) (Fig EV1B). We chose MAPKKK5 for further experiment, because the *mapkkk3* mutation did not affect chitin-induced MAPK activation (Appendix Fig S1).

MAPKKK5 contains a central kinase domain, whereas the N- and C-terminal domains did not possess any known motifs (Fig 1A). Yeast two-hybrid experiments indicated that PBL27 interacted with the C-terminal domain of MAPKKK5, but not the other domains or the full-length protein (Fig 1B and Appendix Fig S2). MAPKKK5 did not interact with related RLCKs, PBL1, BIK1, and PBS1 (Appendix Fig S3). Expression of MAPKKK5 was induced by chitin ((GlcNAc)₇) (Fig EV2A). However, the expression level was very low, because a large number of PCR cycles were required to detect the transcripts. This result was consistent with the publicly available *Arabidopsis* eFP Browser microarray database (<http://www.bar.utoronto.ca/efp/cgi-bin/efpWeb.cgi>) showing extremely low expression levels of MAPKKK5 in most of *Arabidopsis* tissues.

To address whether MAPKKK5 is involved in chitin-induced MAPK activation, we prepared two homozygous lines of *mapkkk5* mutants, *mapkkk5-1* (SAIL_1219_E11) and *mapkkk5-2* (SALK_122847) (Fig EV2B). Transcripts of MAPKKK5 were not detected in these two mutants by semiquantitative RT–PCR (Fig EV2C). These *mapkkk5* mutants were morphologically similar to wild type (Fig EV2D).

We treated these *mapkkk5* mutants with chitin and analyzed the MAPK activation by immunoblot with α -pMAPK. The chitin-induced activation of MPK3, MPK4, and MPK6 was strongly reduced in both mutants (Fig 1C). Furthermore, the loss of the MAPK activation was complemented by expressing C-terminally FLAG-tagged MAPKKK5 from its native promoter (Fig 1D and Appendix Fig S4A). However,

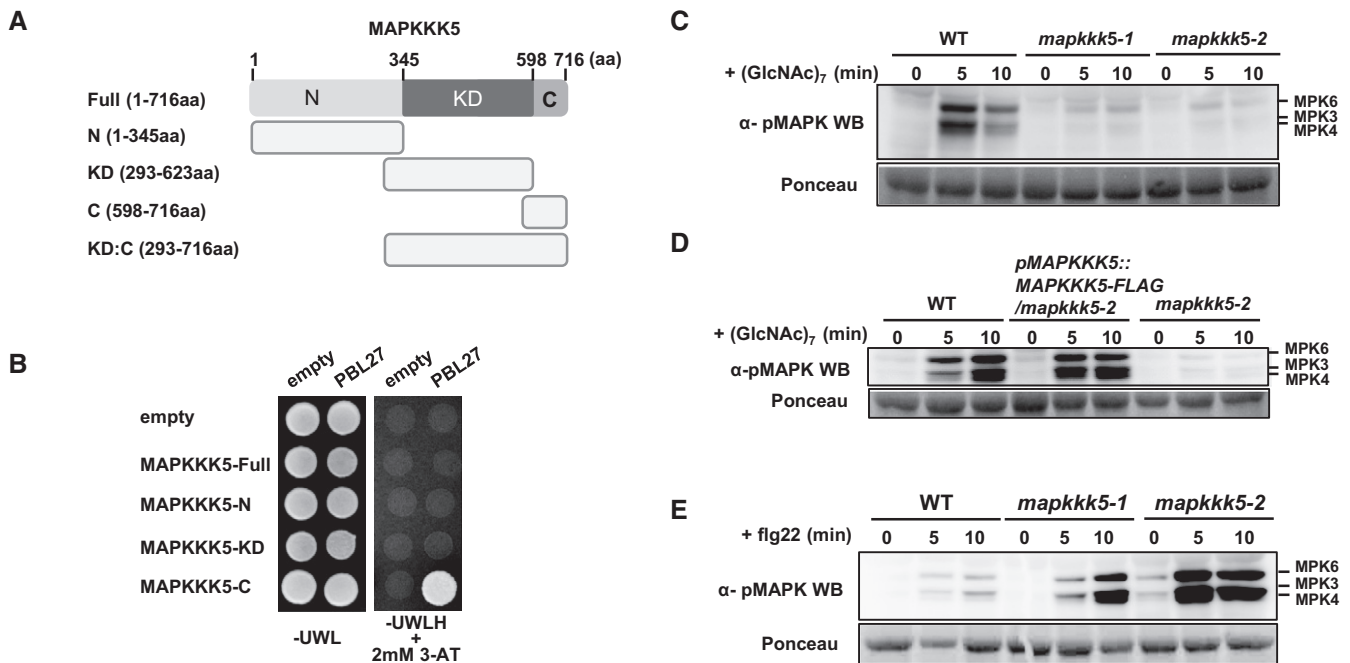


Figure 1. MAPKKK5 regulates chitin-induced MAPK activation.

- A Schematic diagram of MAPKKK5 constructs. N: N-terminal domain, KD: kinase domain, C: C-terminal domain.
 B MAPKKK5-C interacts with PBL27 in yeast two-hybrid experiments. The growth of yeast colonies on plates (-UWLH) lacking uracil (U), leucine (L), tryptophan (W), and histidine (H) with 2 mM 3-aminotriazole (3-AT) indicates a positive interaction.
 C Chitin-induced MAPK activation was analyzed by immunoblots with α -pMAPK.
 D Complementation of chitin-induced MAPK activation in *mapkkk5* mutants by expression of *MAPKKK5-FLAG*. MAPK activation was analyzed by immunoblots with α -pMAPK.
 E Flg22-induced MAPK activation was analyzed by immunoblots with α -pMAPK.

Data information: Experiments (B–E) were performed three times with similar results.

the MAPKKK5-FLAG protein could not be detected by immunoblot with α -FLAG. Therefore, we also produced transgenic *mapkkk5* plants carrying *pMAPKKK5::MAPKKK5-GFP* (Appendix Fig S4B). Expression of *MAPKKK5-GFP* also complemented the *mapkkk5* phenotype (Appendix Fig S4C). However, we failed to detect the MAPKKK5-GFP protein by immunoblot with α -GFP, even though the protein was enriched by immunoprecipitation with α -GFP from large amounts of tissue samples. The GFP fluorescence was also undetectable in the plants. These results suggested that the protein level of MAPKKK5 is very low in the cells, although the level is enough for its *in vivo* biological function.

To examine whether MAPKKK5 is involved in flg22-induced MAPK activation, we treated the *mapkkk5* mutants with flg22. We observed enhanced activation of these MAPKs in the *mapkkk5* mutants (Fig 1E), suggesting that MAPKKK5 may negatively regulate flg22-induced MAPK activation.

mapkkk5 mutants compromise immune responses

We investigated chitin-induced immune responses and disease resistance in the *mapkkk5* mutants. Chitin-induced callose deposition was significantly reduced in the *mapkkk5* mutants (Fig 2A). The *mapkkk5* mutation did not influence ROS production (Fig 2B), consistent with the *pbl27* mutants (Shinya et al, 2014). As reported

previously, *lyk5*, *cerk1*, and *pbl27* mutations reduce resistance to the fungal pathogen *Alternaria brassicicola* (Miya et al, 2007; Cao et al, 2014; Shinya et al, 2014). The *mapkkk5* mutants were inoculated with *A. brassicicola*, and the disease lesions were evaluated compared with wild-type plants. The *mapkkk5* mutants developed larger disease lesions than the wild type, as also observed in the *pbl27-1* mutant (Fig 2C).

To understand MAPKKK5-mediated transcriptional regulation, we carried out global transcriptional profiling by RNA-seq analysis. Totally 12,992 genes were significantly up- or downregulated in wild type at 3 h after chitin treatment (q -value < 0.05; Fig 2D). Among them, the expression patterns of 656 genes were altered in *mapkkk5* compared with wild type, which were shown in the scatter plot (Fig 2D). Motif enrichment analysis using 319 genes showing reduced induction or suppression of gene expression in *mapkkk5* identified the *cis* elements for WRKY, NAC and heat-shock transcription factors (Appendix Fig S5). Among 6,380 genes whose expression was induced or suppressed more than twofold in wild type by chitin, 339 genes showed reduced induction or suppression in *mapkkk5* compared with wild type (Fig 2E and Table EV1), which was confirmed by quantitative RT-PCR analysis of selected genes (Fig 2F). These results indicate that MAPKKK5 regulates chitin-triggered transcriptional reprogramming.

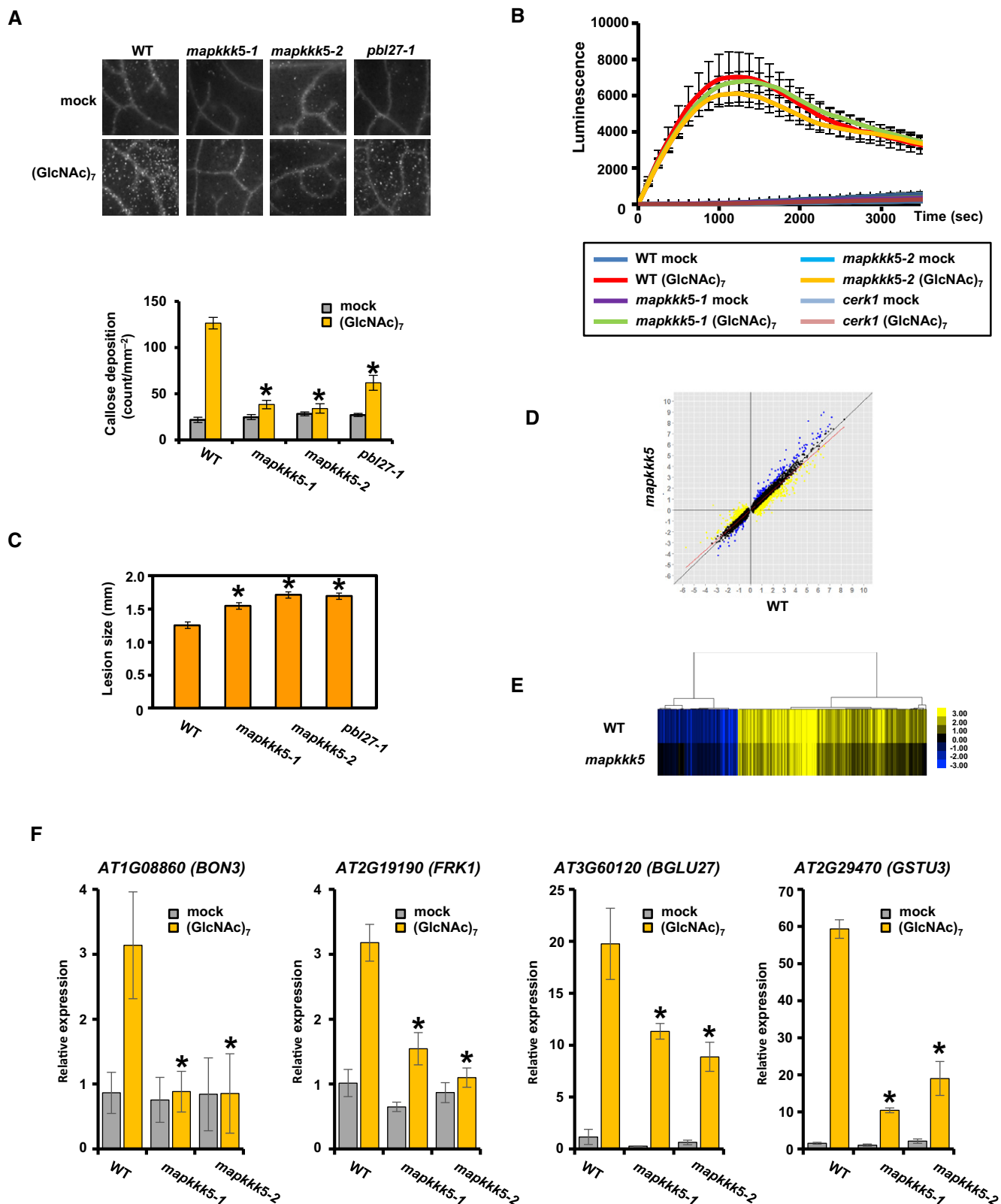


Figure 2.

Figure 2. MAPKKK5-mediated immune response and disease resistance.

- A Chitin-induced callose deposition in the *mapkkk5* mutants. Seedlings were analyzed at 18 h after treatment with 10 μ M chitin. Representative pictures from the biological replicates are presented. Data are means \pm SD from three independent biological replicates, where each biological replicate consists of two technical replicates. The asterisks indicate statistically significant differences from the WT controls by Student's *t*-test ($P < 0.05$).
- B Leaf disks were treated with 10 μ M (GlcNAc)₇ in a solution containing 500 μ M L-012 and 10 μ g/ml horseradish peroxidase. ROS production was quantified using a luminescence microplate reader. Data are means \pm SD calculated using three biological replicates, where each biological replicate consisted of two technical replicates.
- C *mapkkk5* mutations reduce resistance to *Alternaria brassicicola*. Lesion sizes were measured 6 days after inoculation. Values are mean \pm SEM, $n \geq 92$. Asterisks indicate significant difference from wild-type controls by Student's *t*-test ($P < 0.01$).
- D Analysis of chitin-induced transcriptional reprogramming in *mapkkk5-1*. Total RNA was extracted from seedlings treated with mock or 40 μ M chitin for 3 h and analyzed by RNA-seq. Genes that are significantly induced or suppressed by chitin in the wild type were selected (q -value < 0.05 ; 12,992 genes). The log₂ fold changes in the selected genes compared with mock in the wild type and *mapkkk5-1* were plotted. Yellow and blue dots indicate genes that show reduced induction or suppression (506 genes) or enhanced induction or suppression (151 genes) in *mapkkk5-1* compared with the wild type, respectively. The slope of the linear regression line (red) indicates that the overall transcriptional response is weakened in *mapkkk5-1* compared with the wild type. As a comparison, the line $y = x$ (black) is shown. For more details, see the Materials and Methods.
- E A heatmap showing MAPKKK5-dependent genes. Genes showing reduced induction or suppression in *mapkkk5-1* compared with the wild type were selected as described in the Materials and Methods (339 genes). The log₂ fold changes in the selected genes compared with mock were subjected to hierarchical clustering analysis. Yellow indicates positive values, blue indicates negative values, and black indicates zero: see the color scale.
- F Expression patterns of representative MAPKKK5-dependent genes. qRT-PCR analysis of defense-related genes in 8-day-old seedlings exposed to 40 μ M (GlcNAc)₇ for 3 h. Data are shown as the average of three independent biological replicates \pm SD. The asterisks indicate statistically significant differences from the WT controls by Student's *t*-test ($P < 0.05$).

PBL27 interacts with MAPKKK5 in planta

Because the MAPKKK5 proteins could not be detected in *Arabidopsis* plants, we transiently expressed MAPKKK5-GFP under the control of native or *CaMV35S* promoters in *Nicotiana benthamiana* (*Nb*). The expression of MAPKKK5-GFP induced cell death in *Nb* leaves (Fig EV3A). Cell death induced by *p35S::MAPKKK5-GFP* appeared earlier compared with that of *pMAPKKK5::MAPKKK5-GFP*. The MAPKKK5 proteins were detected by immunoblots with α -GFP using total protein purified from leaves expressing MAPKKK5-GFP under the control of the *CaMV35S* promoter but not the native promoter before the appearance of the cell death (Fig EV3B). To analyze the subcellular localization of MAPKKK5, we expressed MAPKKK5-GFP in *Nb* leaves and purified soluble and microsomal fractions. MAPKKK5-GFP was detected in both the microsomal and soluble fractions (Fig 3A). Consistent with this result, the plasmolysis experiment indicated the GFP fluorescence of MAPKKK5 was detected at cytosol and plasma membrane (PM) in *Nb* leaves (Fig 3B).

To examine the *in vivo* interaction between PBL27 and MAPKKK5, PBL27-HA and MAPKKK5-GFP were co-expressed in *Nb* leaves. However, the accumulation level of the PBL27-HA protein was very low in the presence of MAPKKK5-GFP (Fig 3C). Therefore, we generated a kinase-inactive mutant MAPKKK5^{K375M} by substitution of lysine at position 375 with methionine. K375 is a conserved ATP binding site, and this mutation is known to abolish kinase activity (del Pozo *et al.*, 2004). Expression of MAPKKK5^{K375M}-GFP did not induce cell death (Fig EV3C). We detected both MAPKKK5^{K375M}-GFP and PBL27-HA by the immunoblots in *Nb* leaves (Fig 3C). MAPKKK5^{K375M}-GFP was also localized in microsomal fraction (Fig 3D). The co-immunoprecipitation assays with α -GFP were carried out using the microsomal fractions purified from *Nb* leaves expressing PBL27-HA and MAPKKK5^{K375M}-GFP, because both proteins were enriched in the microsomal fraction. PBL27-HA was co-immunoprecipitated with MAPKKK5^{K375M}-GFP (Fig 3E). The interaction of PBL27 with MAPKKK5 was also analyzed by bimolecular fluorescence complementation (BiFC) experiments (Fig 3F). MAPKKK5^{K375M} was tagged with the N-terminal domain of Venus (MAPKKK5^{K375M}-Vn), and PBL27 was tagged with the C-terminal

domain of Venus (PBL27-Vc). A FLS2-associated RLCK, BIK1, was also used in this experiment. Co-expression of MAPKKK5^{K375M}-Vn and PBL27-Vc did not induce cell death in *Nb* leaves, whereas cell death was observed by expression of MAPKKK5-Vn and PBL27-Vc (Fig EV3D). The fluorescence was detected by co-expression of MAPKKK5^{K375M}-Vn with PBL27-Vc but not BIK1-Vc (Fig 3F). In addition, the plasmolysis experiment indicated that the fluorescence was localized at the PM, demonstrating that PBL27 interacts with MAPKKK5 at the PM where CERK1 and PBL27 form the complex (Shinya *et al.*, 2014).

The interaction between MAPKKK5 and PBL27 was also analyzed by transient expression in *Arabidopsis* protoplasts. The accumulation level of MAPKKK5^{K375M}-GFP was much higher than that of MAPKKK5-GFP (Fig 4A). In addition, expression of MAPKKK5-GFP reduced the level of PBL27-HA (Fig 4B), as found in *Nb* leaves (Fig 3C). Treatment with a proteasome inhibitor MG132 resulted in increased protein levels of PBL27 and MAPKKK5 (Fig 4C), suggesting that the protein levels of PBL27 and MAPKKK5 may be regulated in a proteasome-dependent manner.

MAPKKK5^{K375M}-GFP was co-immunoprecipitated with PBL27-HA (Fig 4D). Furthermore, the BiFC experiments displayed the interaction of MAPKKK5^{K375M} with PBL27 but not BIK1 at the PM in *Arabidopsis* protoplasts (Fig 4E), indicating that PBL27 forms the complex with MAPKKK5 at PM. Furthermore, we examined whether the complex formation was affected by chitin signaling. The chitin elicitation induced the disassociation of PBL27-HA and MAPKKK5^{K375M}-GFP interaction (Fig 4F). However, the disassociation did not occur by treatment with flg22. These data suggest that MAPKKK5 may be released from PBL27 after ligand perception by the CERK1 complex.

PBL27 directly phosphorylates MAPKKK5

To analyze whether PBL27 phosphorylates MAPKKK5, we carried out *in vitro* kinase assay. PBL27 directly phosphorylated only the C-terminal domain of MAPKKK5 (Fig 5A). In contrast, none of the MAPKKK5 fragments were phosphorylated by BIK1 (Fig 5B), whereas BIK1 phosphorylated the N-terminal domain of RBOHD as

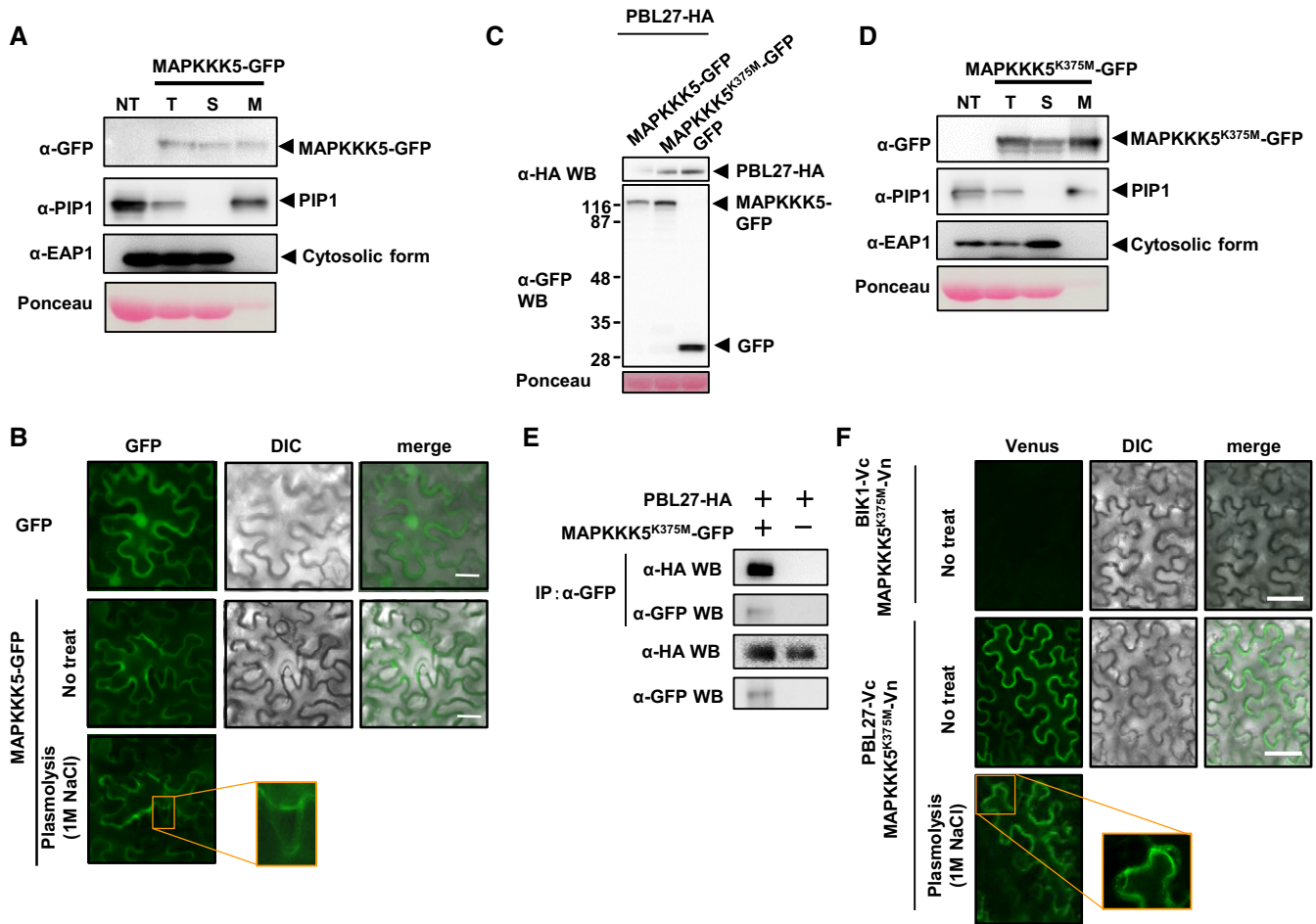


Figure 3. MAPKKK5 interacts with PBL27 at plasma membrane.

- A The MAPKKK5-GFP protein was detected in the membrane fraction. The total (T), soluble (S), and microsomal membrane (M) fractions purified from *Nb* leaves expressing MAPKKK5-GFP were used for immunoblots with antibodies against GFP, PM-localized aquaporin PIP1, and cytosolic ascorbate peroxidase EAP1.
- B Subcellular localization of MAPKKK5-GFP and GFP in *Nb* leaves. The results were photographed at 38 hpi. Scale bars = 50 μ m.
- C Detection of MAPKKK5-GFP and PBL27-HA transiently expressed in *Nb* leaves. Total proteins were purified from *Nb* leaves at 38 hpi.
- D Localization of MAPKKK5^{K375M}-GFP was analyzed by using total (T), soluble (S), and microsomal membrane (M) fractions purified from *Nb* leaves expressing MAPKKK5^{K375M}-GFP.
- E Co-immunoprecipitation assays show that MAPKKK5^{K375M}-GFP forms the complex with PBL27-HA in *Nb* leaves. The microsomal fractions purified from *Nb* leaves co-expressing MAPKKK5^{K375M}-GFP and PBL27-HA at 48 hpi were used for co-immunoprecipitation with α -GFP.
- F Visualization of the interaction between PBL27 and MAPKKK5^{K375M} by bimolecular fluorescence complementation (BiFC) analysis in *Nb* leaves. The results were photographed at 38 hpi. Venus fluorescence indicates the interaction between PBL27 and MAPKKK5^{K375M}. Scale bars = 50 μ m.

previously reported (Kadota *et al*, 2014). To determine the amino acid residues of MAPKKK5 phosphorylated by PBL27, the C-terminal domain of MAPKKK5 was phosphorylated *in vitro* by PBL27, and subjected to liquid chromatography–tandem mass spectrometry. We identified a total of six amino acid residues, S-617, S-622, S-658, S-660, T-677, and S-685, which were phosphorylated by PBL27 (Fig 5C and Appendix Fig S6). To examine the phosphorylation level of each amino acid residue by PBL27, each of the six residues was substituted with alanine. The *in vitro* kinase assay indicated that the phosphorylation level by PBL27 was strongly decreased by the S622A mutation, although other mutations, except for T677A, slightly reduced phosphorylation (Fig 5D). In addition, all of the phosphorylated sites were substituted with alanine, and the resultant protein (MAPKKK5-C^{6xA}) was used for *in vitro* kinase assays.

The phosphorylation of MAPKKK5-C by PBL27 was almost completely lost by these substitutions (Fig 5E), although these alanine substitutions did not affect the interaction between PBL27 and MAPKKK5-C (Fig 5F and Appendix Fig S2).

To elucidate whether the six residues phosphorylated by PBL27 is required for chitin-induced MAPK activation, we introduced *pMAPKKK5::MAPKKK5^{6xA}-FLAG* into the *mapkkk5* mutant (Appendix Fig S4A). Expression of MAPKKK5^{6xA} did not fully complement the chitin-induced activation of MPK3, MPK4, and MPK6 (Fig 6A and Appendix Fig S7A) and callose deposition (Fig 6B) in the *mapkkk5* mutant. We also produced transgenic plants expressing MAPKKK5^{6xA}-GFP. Consistent with the results of the *pMAPKKK5::MAPKKK5^{6xA}-FLAG* plants, expression of MAPKKK5^{6xA}-GFP only partially complemented the chitin-induced

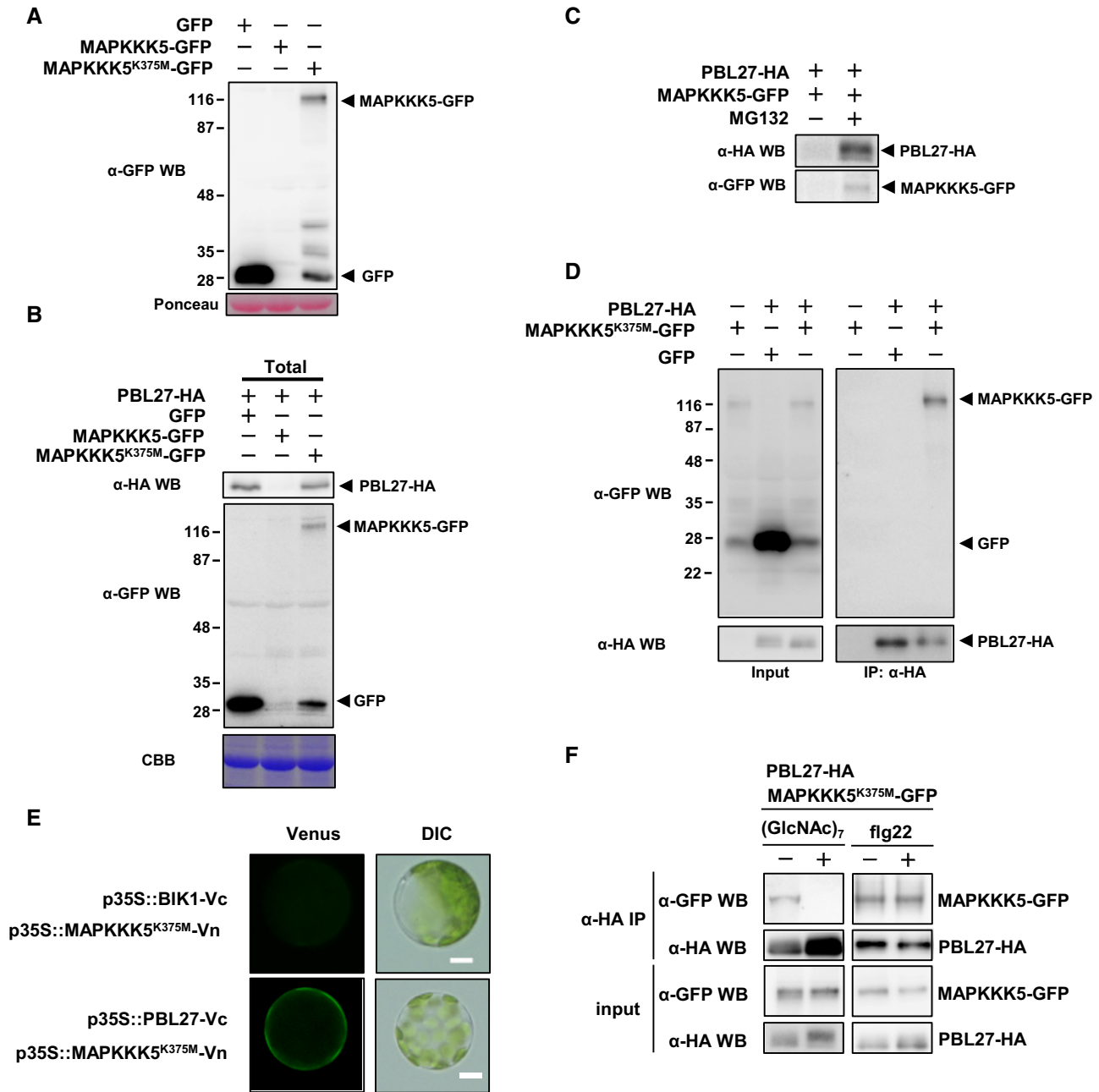


Figure 4. MAPKKK5 disassociates from PBL27 after chitin perception.

A Detection of MAPKKK5-GFP and MAPKKK5^{K375M}-GFP transiently expressed in *Arabidopsis* protoplasts.
 B Expression of MAPKKK5-GFP reduces the level of PBL27. CBB, Coomassie brilliant blue.
 C *Arabidopsis* protoplasts expressing PBL27-HA and MAPKKK5-GFP were treated with 30 μM MG132 for 3 h and subjected to immunoblots with α-HA and α-GFP.
 D The co-immunoprecipitation assay shows that PBL27 forms the complex with MAPKKK5 in *Arabidopsis* protoplasts. Total proteins purified from protoplasts co-expressing PBL27 and MAPKKK5 were subjected to immunoprecipitation with α-HA.
 E Visualization of the interaction between PBL27 and MAPKKK5^{K375M} by BiFC analysis in *Arabidopsis* protoplasts. FLS-associated RLCK BIK1 was also used for this assay. Venus fluorescence indicates interaction between PBL27 and MAPKKK5^{K375M}. Scale bars = 10 μm.
 F The disassociation of PBL27-MAPKKK5 interaction after chitin treatment in *Arabidopsis* protoplasts. Protoplasts were co-transfected with MAPKKK5^{K375M}-GFP and PBL27-HA, stimulated with or without 10 μM chitin or 1 μM flg22 for 10 min and subjected to the co-immunoprecipitation assay.

Data information: Experiments (A–F) were performed three times with similar results.

activation of MPK3, MPK4 and MPK6 (Appendix Fig S7B). Although the MAPKKK5^{6xA}-GFP protein was unable to be detected from the transgenic plants, *Arabidopsis* protoplast expression transient assay

indicated that the protein levels of MAPKKK5 were not affected by these alanine substitutions (Fig 6C), and MAPKKK5^{6xA} interacted with PBL27, but not BIK1 at PM (Fig 6D). Furthermore, same results

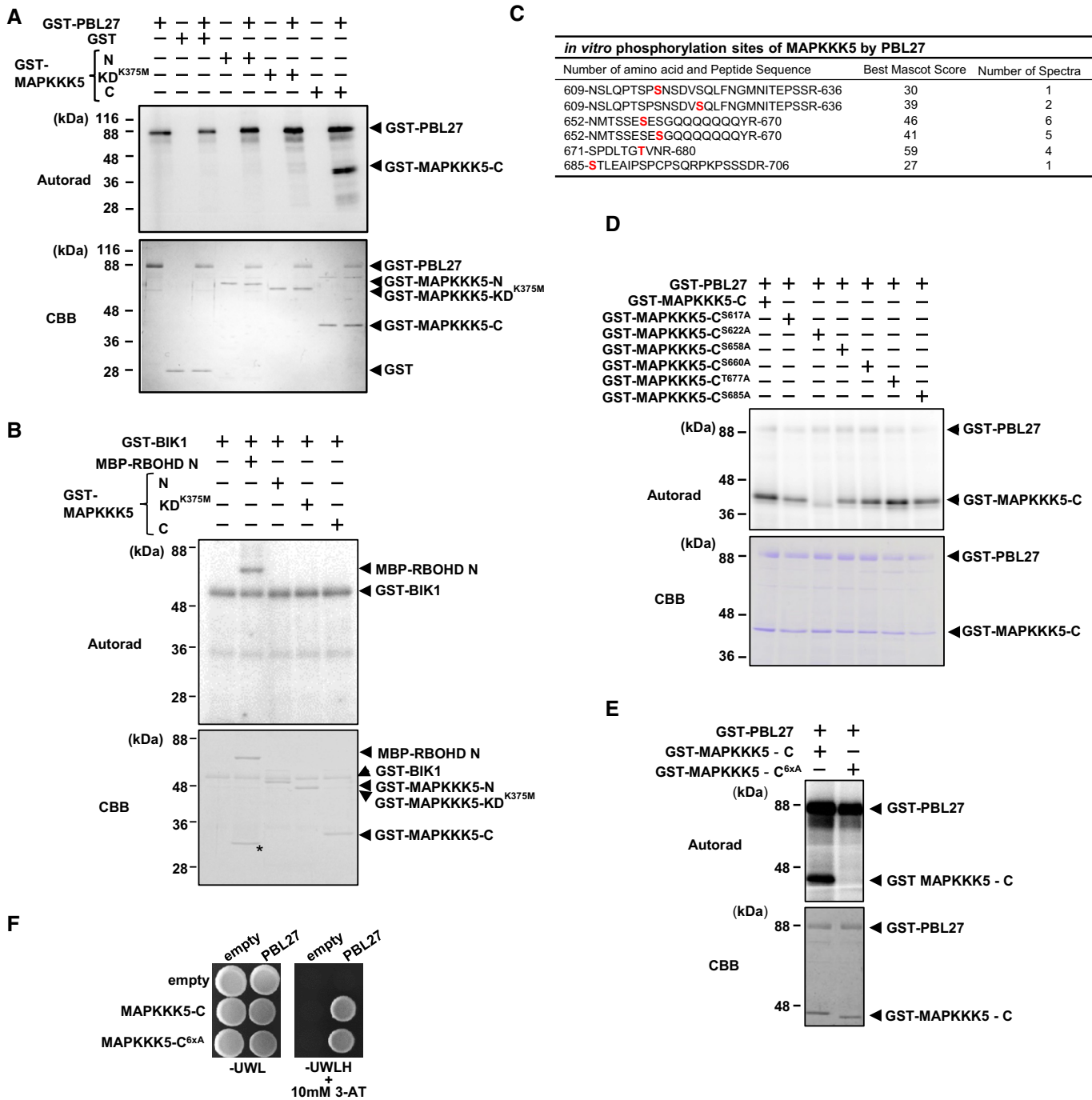


Figure 5. PBL27 phosphorylates the C-terminal domain of MAPKKK5.

- A PBL27 phosphorylates MAPKKK5-C *in vitro*. The *in vitro* phosphorylation reaction was carried out using [³²P]γ-ATP, and the phosphorylated proteins were detected by autoradiography. CBB, Coomassie brilliant blue.
- B BIK1 does not phosphorylate MAPKKK5-C *in vitro*. RBOHD was used as a positive control. Asterisk indicates artificial bands.
- C Identification of amino acid residues of MAPKKK5 phosphorylated by PBL27. The C-terminal domain of MAPKKK5 was phosphorylated by PBL27 *in vitro* and subjected to LS-MS/MS analysis. All MS/MS spectra of phosphorylated peptides were validated manually. The amino acid residues phosphorylated by PBL27 are shown in red.
- D The S622A mutation strongly reduces phosphorylation by PBL27. Each phosphorylation site was substituted by alanine and subjected to the *in vitro* phosphorylation assays.
- E PBL27 does not phosphorylate MAPKKK5-C^{6xA} *in vitro*. The *in vitro* phosphorylation reaction was carried out using [³²P]γ-ATP, and the phosphorylated proteins were detected by autoradiography.
- F PBL27 interacts with MAPKKK5-C^{6xA} in yeast two-hybrid experiments. The growth of yeast colonies on plates (-ULWH) lacking uracil (U), leucine (L), tryptophan (W), and histidine (H) with 10 mM 3-AT indicated a positive interaction.

were also obtained by agroinfiltration assay using the *Nb* leaves (Fig EV4). Thus, it is unlikely that the defects in MAPK activation and callose deposition in the *pMAPKKK5::MAPKKK5^{6xA}-FLAG* or *GFP/mapkkk5* plants are caused by mislocalization and low protein stability of MAPKKK5^{6xA}. These data indicate that the phosphorylation of MAPKKK5 at the mutated six residues by PBL27 is essential for MAPKKK5-mediated activation of MPK3, MPK4 and MPK6.

Identification of a possible phospho-signaling pathway of chitin-induced MAPK activation

During a study of the interaction between PBL27 and MAPKKK5, we found that PBL27 did not interact with MAPKKK5-KD^{K375M}:C (293–716aa) in yeast (Figs 1A and 7A, and Appendix Fig S2). PBL27 hardly phosphorylated MAPKKK5-KD^{K375M}:C (Fig 7B, lane 4). However, addition of the intracellular kinase domain of CERK1 (CERK1:IC) to the kinase assay strongly enhanced the phosphorylation of MAPKKK5-KD^{K375M}:C by PBL27 (Fig 7B, lane 6). In contrast, PBL27 did not phosphorylate MAPKKK5-KD^{K375M}:C^{6xA} even in the presence of CERK1:IC (Fig 7B, lane 5). CERK1:IC did not directly phosphorylate MAPKKK5-C (Fig 7C). These results suggest that PBL27-mediated phosphorylation of the C-terminal domain but not the kinase domain of MAPKKK5 is dependent on CERK1.

Previous studies indicate that the RLKs such as BAK1 and OsCERK1 phosphorylate Ser and/or Thr residues conserved in the activation loops of the RLCK family (Lu *et al*, 2010; Zhang *et al*, 2010; Yamaguchi *et al*, 2013). To test whether CERK1 phosphorylates the corresponding residues S-244, T-245, and S-250 at the activation loop of PBL27, these residues of kinase-inactive PBL27^{K112E} (Shinya *et al*, 2014) were substituted with alanine, and the resultant protein (PBL27^{K112E, 3xA}) was used for *in vitro* kinase assay (Fig 7D). The phosphorylation of PBL27 by CERK1 was greatly reduced by these substitutions. Because phosphorylation of the activation loop of protein kinases is known to determine substrate access (Huse & Kuriyan, 2002), it is possible that the phosphorylation of these residues by CERK1 may increase the access of PBL27 to MAPKKK5. However, the fact that PBL27 with the alanine substitutions of these residues lost the own kinase activity (Fig 7E) precluded testing whether the phosphorylation at these residues is responsible for enhanced phosphorylation of MAPKKK5 by PBL27. Taken together, it is likely that phosphorylation of PBL27 by CERK1 positively regulates the phosphorylation of MAPKKK5 by PBL27.

MKK4 and MKK5 redundantly function as MAPKKs for MPK3 and MPK6, and MKK1 and MKK2 act upstream of MPK4 (Rasmussen *et al*, 2012). The fact that chitin-induced activation of MPK3, MPK6, and MPK4 was reduced in *mapkkk5* suggests a

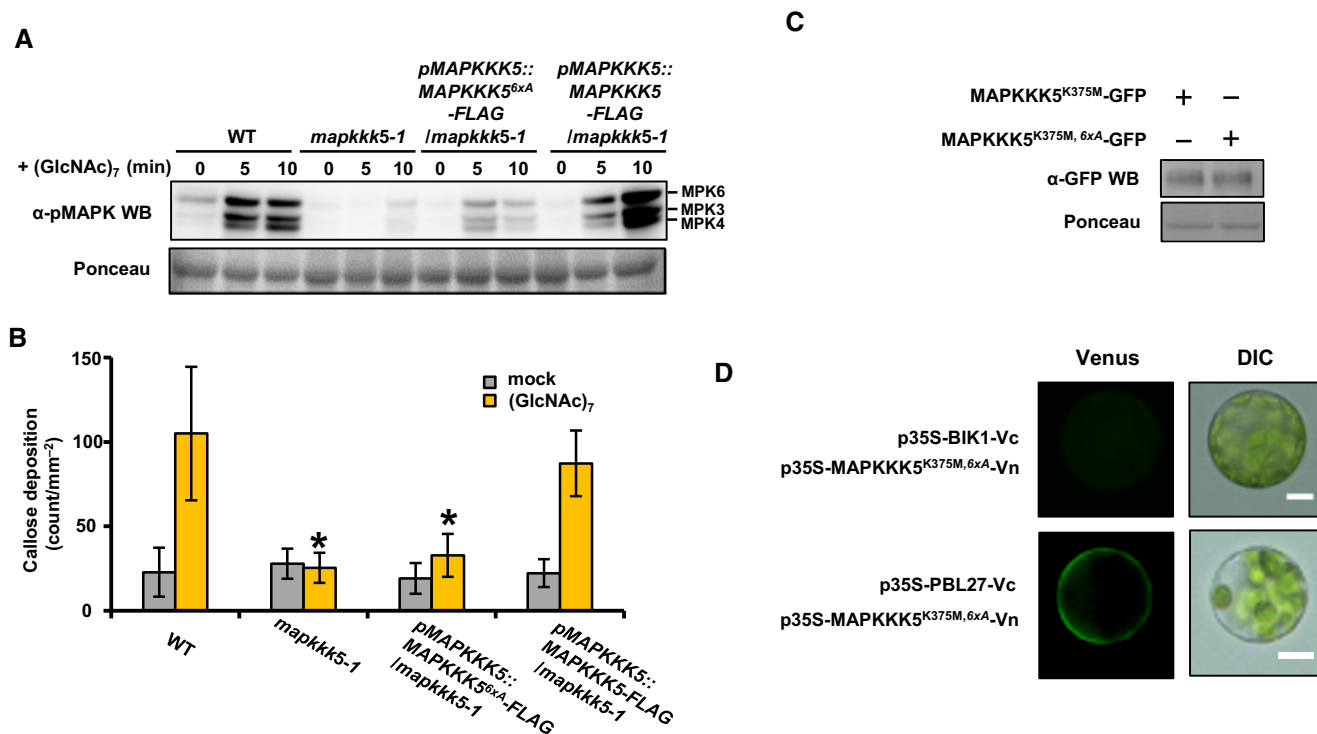


Figure 6. The phosphorylation sites of MAPKKK5 are required for chitin-induced MAPK activation.

- A Chitin-induced MAPK activation in a *mapkkk5* mutant (Line 1) expressing MAPKKK5^{6xA}. MAPK activity was detected using immunoblots with α-pMAPK.
- B Chitin-induced callose deposition in the MAPKKK5^{6xA} plant (Line 1). Seedlings were analyzed at 18 h after treatment with 10 μM chitin. Data are means ± SD from three independent biological replicates, where each biological replicate consists of two technical replicates. The asterisks indicate statistically significant differences from the WT controls by Student's *t*-test ($P < 0.05$).
- C Detection of MAPKKK5^{K375M}-GFP and MAPKKK5^{K375M, 6xA}-GFP transiently expressed in *Arabidopsis* protoplasts.
- D Visualization of interaction between PBL27 and MAPKKK5^{K375M, 6xA} by BiFC analysis in *Arabidopsis* protoplasts. Venus fluorescence indicates interaction between PBL27 and MAPKKK5^{K375M, 6xA}. Scale bars = 10 μm.

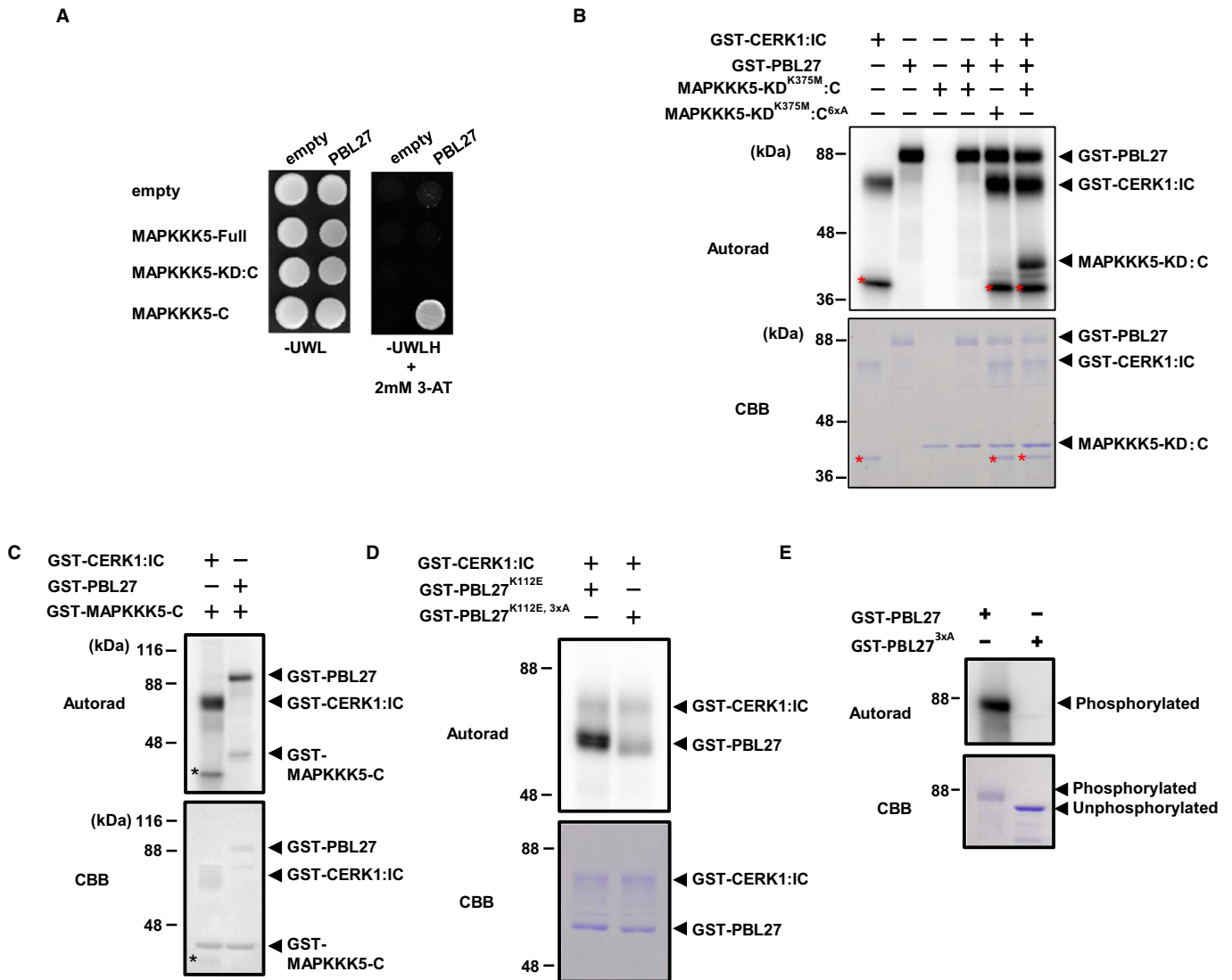


Figure 7. PBL27 phosphorylates MAPKKK5-KD:C in CERK1-dependent manner.

A PBL27 does not interact with MAPKKK5-KD:C in a yeast two-hybrid assay.
B Addition of CERK1 to an *in vitro* kinase assay enhances phosphorylation of MAPKKK5-KD^{K375M}:C by PBL27. Asterisks indicate artificial bands derived from CERK1:IC.
C CERK1 does not phosphorylate the C-terminal domain of MAPKKK5 *in vitro*. The *in vitro* kinase assay was performed with recombinant proteins of GST-PBL27, MAPKKK5-C and the intracellular kinase domain of CERK1 (GST-CERK1:IC). The protein loading control was shown by staining with Coomassie brilliant blue. The *in vitro* phosphorylation reaction was carried out using [³²P]γ-ATP, and the phosphorylated proteins were detected by autoradiography. Asterisks indicate artificial bands.
D The alanine substitution mutations at the residues conserved in the activation loop of reduces the phosphorylation of PBL27 by CERK1:IC. The *in vitro* kinase assay was carried out with recombinant proteins of GST-PBL27^{K112E}, GST-PBL27^{K112E, 3xA}, and CERK1:IC.
E The kinase activity of GST-PBL27^{3xA} was analyzed by the *in vitro* kinase assay using [³²P]γ-ATP.

possibility that MAPKKK5 may interact with all of MKK1, MKK2, MKK4, and MKK5. We carried out BiFC assay using *Arabidopsis* protoplasts to examine *in vivo* interaction between MAPKKK5^{K375M} and these MAPKKs. The BiFC signals indicated that MAPKKK5 interacts with MKK2, MKK4, and MKK5 mainly in the cytosol (Fig 8A), although the interaction between MAPKKK5 and MKK1 was not detected.

The *in vitro* kinase assays were carried out using the kinase-inactive mutants of these MAPKKs. The kinase domain of MAPKKK5 directly phosphorylated MKK4^{K108R} and MKK5^{K99R} (Fig 8B). In the *in vitro* experimental condition, the phosphorylation level of

MKK5^{K99R} by MAPKKK5-KD was much higher than that of MKK4^{K108R}, and MAPKKK5-KD has a low autophosphorylation activity compared with the transphosphorylation of MKK4 and MKK5. In general, MAPKKs are known to be activated through the phosphorylation of two Ser/Thr residues, in a conserved S/TxxxxxS/T motif of the activation loop, by MAPKKs (Ichimura *et al*, 2002). Therefore, we substituted the S/TxxxxxS/T motif residues, T-224/S-230 of MKK4 and T-215/S-221 of MKK5 with alanine. The phosphorylation of MKK4 and MKK5 by MAPKKK5-KD was greatly reduced by the alanine substitutions of the S/TxxxxxS/T motifs (Fig 8C), suggesting that MAPKKK5 is involved in activation

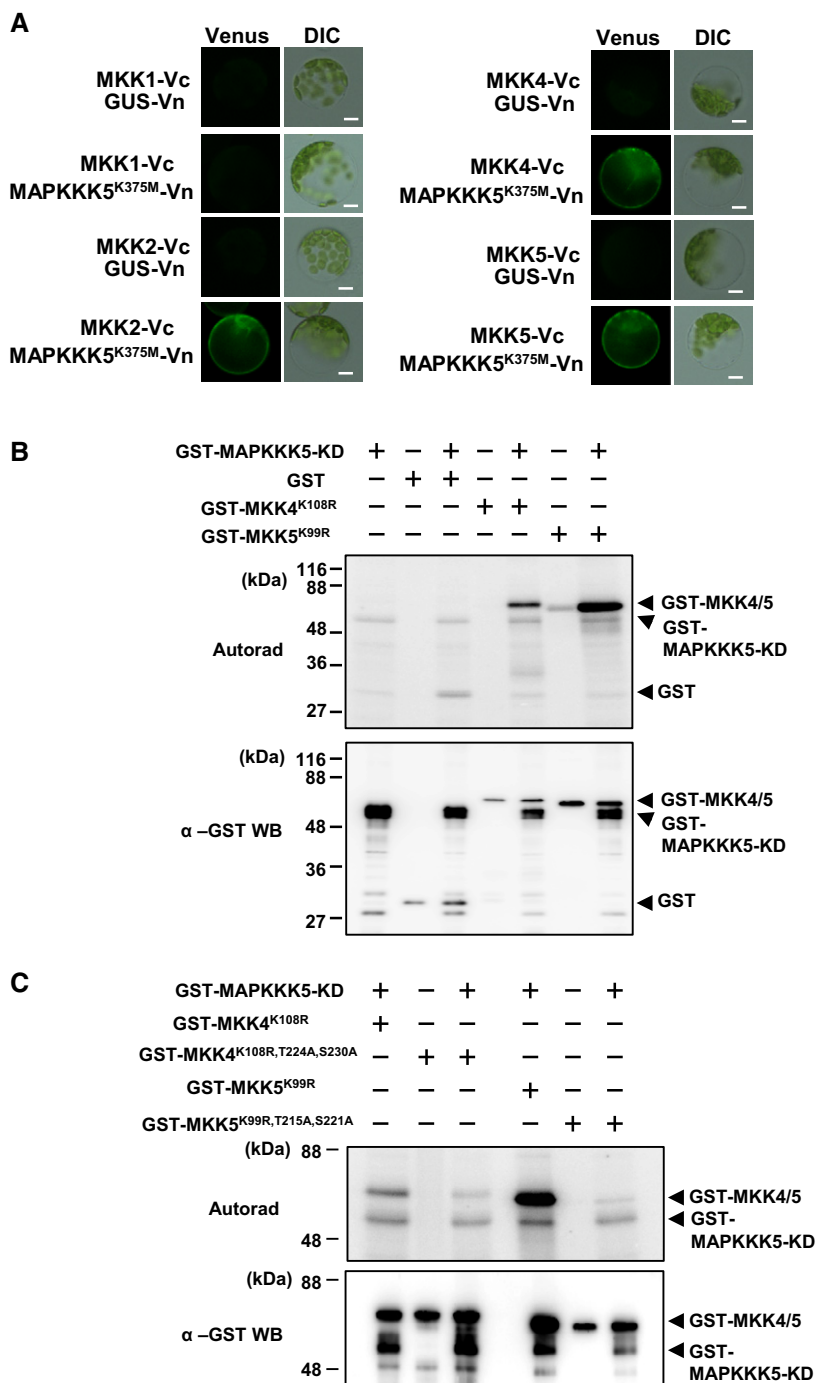


Figure 8. MAPKKK5 phosphorylates the activation loops of MKK4 and MKK5.

A Visualization of interaction between MAPKKK5^{K375M} and MKK1/MKK2/MKK4/MKK5 by BiFC analysis in *Arabidopsis* protoplasts. Venus fluorescence indicates interaction. Scale bars = 10 μm.

B MAPKKK5-KD phosphorylates MKK4 and MKK5 *in vitro*. The *in vitro* phosphorylation reaction was carried out using [³²P]γ-ATP, and the phosphorylated proteins were detected by autoradiography.

C MAPKKK5-KD does not phosphorylate a T224A/S230A mutant of MKK4 or a T215A/S221A mutant of MKK5.

Data information: The above experiments were performed three times with similar results.

of MKK4 and MKK5. In contrast to MKK4 and MKK5, MAPKKK5-KD did not phosphorylate MKK1^{K97R} (Fig EV5A). Although MKK2^{K99R} was slightly phosphorylated by MAPKKK5-KD, the alanine

substitution of the S/TxxxxS/T motif did not influence the phosphorylation level of MKK2^{K99R} (Fig EV5B and C). Thus, the *in vitro* phosphorylation assay did not support the idea that MAPKKK5

regulates activation of MKK1 and MKK2. Altogether, these results suggested at least a possible phospho-signaling pathway consisting of CERK1–PBL27–MAPKKK5–MKK4/MKK5–MPK3/MPK6 (Appendix Fig S8).

Discussion

Plant MAPK cascades have been widely investigated and they have been shown to be activated upon the perception of MAMPs by many PRRs. MAPKs function as pivotal signaling modules to regulate diverse immune responses. Nevertheless, it has not been established how PRRs transmit their activation signals to MAPK cascades (Rasmussen *et al*, 2012). In this study, we discovered that the RLCK PBL27 functions as the MAPKKK kinase to connect activation of the chitin receptor complex CERK1-LYK5 to the canonical MAPK cascade.

The Co-IP and BiFC experiments showed that MAPKKK5 interacts with PBL27 at PM. However, the interaction with full-length MAPKKK5 could not be observed in the yeast two-hybrid and *in vitro* experiments; instead, only the C-terminal domain of MAPKKK5 interacts with PBL27. The discrepancy may be explained by the possibility that additional components such as scaffold proteins may be required for the complex formation of PBL27 and MAPKKK5. In addition, the *in vitro* kinase assay indicates that the phosphorylation of MAPKKK5 by PBL27 was strongly enhanced in the presence of CERK1, implying that the phosphorylation of the activation loop of PBL27 by CERK1 may enhance the access of PBL27 to the C-terminal domain of MAPKKK5 in the complex.

The present data obtained by the *in vitro* phosphorylation and *in vivo* interaction assays, and the genetic experiments with the alanine substitution mutants indicate the phosphorylation of MAPKKK5 by PBL27 in a CERK1-dependent manner. To gain direct evidence for the phosphorylation *in vivo*, we carried out phosphoproteome analysis by liquid chromatography–mass spectrometry to quantitatively examine the chitin-induced *in vivo* phosphorylation levels of MAPKKK5. However, we failed it because of technical difficulty caused by extremely low expression of MAPKKK5 in plants. On the other hand, the chitin perception induced the disassociation of PBL27 and MAPKKK5, demonstrating a sequential *in vivo* event in the physiological signaling pathway of CERK1-PBL27-MAPKKK5.

Three RLCKs, BIK1, PBL1, and BSK1, are downstream components of the flagellin receptor complex FLS2/BAK1 (Lu *et al*, 2010; Zhang *et al*, 2010; Shi *et al*, 2013). However, the *bik1*, *pbl1*, and *bsk1* mutations did not influence MAPK activation. In contrast, FLS2-mediated MAPK activation is suppressed by *Xanthomonas campestris* effector AvrAC that inhibits the activities of RLCKs by uridylylating conserved phosphorylation sites in the activation loop (Feng *et al*, 2012), suggesting that unidentified RLCKs targeted by AvrAC may transmit the signal from FLS2 to these MAPKs. Very recently, the *bik1 pbl1* double mutant has been reported to reduce the MAPK activation induced by the perception of the endogenous PROPEP peptides with the LRR-RLKs PEPR1/PEPR2 (Yamada *et al*, 2016). These data suggest that the RLCK family may be the main linking elements between cell surface receptors and intercellular MAPK signaling.

In response to FLS2-mediated ligand perception, BIK1 phosphorylates NADPH oxidase RBOHD, leading to the production of

ROS (Ao *et al*, 2014; Kadota *et al*, 2014). However, as mentioned above, BIK1 is not involved in MAPK activation downstream of FLS2 (Feng *et al*, 2012). In contrast, PBL27 regulates MAPK activation through the phosphorylation of MAPKKK5, but not ROS production (Shinya *et al*, 2014). Chitin-induced ROS production is regulated by the phosphorylation of RBOHD by BIK1 in the same way as FLS2-mediated signaling (Kadota *et al*, 2014). Thus, it appears that MAPK activation and ROS production are independently mediated by different RLCKs downstream of FLS2 and CERK1 in *Arabidopsis*. Interestingly, silencing of *OsRLCK185* reduces both the MAPK activation and ROS production induced by chitin in rice (Yamaguchi *et al*, 2013). How the specificities of interactions between RLCK and MAPKKK or between RLCK and RBOH are determined is an intriguing question.

Arabidopsis heterotrimeric G-protein complexes and receptor for activated C kinase 1 (RACK1) were reported to participate in activation of the MAPK cascade induced by pathogen-secreted proteases (Cheng *et al*, 2015), although the receptors for the proteases are unknown. However, FLS2-mediated MAPK activation does not involve the heterotrimeric G-protein and RACK1 (Cheng *et al*, 2015), demonstrating at least two different pathways of the MAPK activation downstream of PRRs.

Chitin-induced MAPK activation was strongly reduced in *mapkkk5*. In contrast, the *mapkkk5* mutation significantly enhanced flg22-induced MAPK activation. While it shows that MAPKKK5 functions as a positive regulator specifically during chitin perception, it suggests that MAPKKK5 might have different roles on other pathways. Recently, MAPKKK7 has been reported to negatively regulate MPK6 during flg22 signaling (Mithoe *et al*, 2016). Thus, it is possible that MAPKKK5 possesses a similar negative function as MAPKKK7 in flg22-induced pathway. In turn, the enhanced MPK activation could also be part of a compensation mechanism, where the absence of MAPKKK5 somehow increases the abundance/access of other MAPKKKs that activate MPKs during flg22 signaling. Similarly, this could be caused by enhanced levels of the components of flg22-recognition receptor such as FLS2 and BAK1 in *mapkkk5* mutant as found in *acd6* mutant (Tateda *et al*, 2014).

Overexpression of MAPKKK5 induces cell death in *Nb* leaves. As mentioned above, since MAPKKK5 may negatively regulate flg22-induced MAPK activation, it is possible that cell death induced by overexpression of MAPKKK5 would be caused by inhibition of flg22-induced MAPK activation which would trigger the activation of NB-LRR-type disease resistance proteins guarding components of the MAPK cascades such as the NB-LRR protein SUMM2 sensing the MPK4 activity (Zhang *et al*, 2012).

Chitin-induced MPK4 activation was also reduced in *mapkkk5*. Although MPK4 is known to be activated through MKK1 and MKK2, we could not obtain the evidence that MAPKKK5 regulates MPK4 activation through MKK1 and MKK2. In the flg22 response, it has been well investigated that MEKK1 activates the MKK1/MKK2–MPK4 pathway (Meng & Zhang, 2013). Although whether MEKK1 is involved in chitin signaling is unknown, it is possible that MAPKKK5 may cooperate with MEKK1 in chitin signaling. Additionally, there may be a possibility that a MAPKK other than MKK1/2 could phosphorylate MPK4 during chitin signaling.

In addition to immunity, plant development and growth are also regulated by the MAP kinase cascades activated by the perception of

hormones and secreted peptides by cell surface RLKs (Meng *et al*, 2015). It is possible that the RLCK family connects receptors and MAPK cascades in developmental processes. In fact, recent genetic experiments on plant embryogenesis indicated that the *Arabidopsis* RLCK SSP regulates MAPK activation mediated by the MAPKKK YODA (Bayer *et al*, 2009; Costa *et al*, 2014). Further study is required to reveal the molecular basis of how this broad diversity of cell surface receptors is tied to what is likely to be a redundant set of diverse RLCKs, and how these engage the broad diversity of MAPKKs in plants to mediate MAPK cascade activation in plant immunity and development.

Materials and Methods

Plant materials

Arabidopsis plants were grown in a 16-h light/8-h dark cycle at 22°C (light) or 20°C (dark). Two *MAPKKK5* T-DNA insertion mutants in a Col-0 background were obtained from the *Arabidopsis* Biological Resource Center and designated as *mapkkk5-1* (SAIL_1219_E11) and *mapkkk5-2* (SALK_122847), respectively. *pbl27-1* (GABI_01C07) was described previously (Shinya *et al*, 2014). The promoter region of *MAPKKK5* was amplified from genomic DNA using specific primers (Appendix Table S1). The promoter region was combined with the open reading frame of *MAPKKK5*, and then the resultant fragment (*pMAPKKK5::MAPKKK5*) was subcloned into a pENTR/D-TOPO vector (Invitrogen). The *pMAPKKK5::MAPKKK5* DNA fragment was transferred into the binary vector pGWB10 or pGWB4 (Nakagawa *et al*, 2007) to generate a construct for the expression of *MAPKKK5-FLAG* or *MAPKKK5-GFP*, respectively, under the control of the native *MAPKKK5* promoter (*pMAPKKK5*) in *Arabidopsis*. To generate transgenic *Arabidopsis* plants, immature floral buds of *Arabidopsis* plants were infected with *Agrobacterium tumefaciens* *EHA101* carrying each construct using the floral-dip method (Clough & Bent, 1998).

Plasmid constructs

DNA fragments of *MAPKKK5*, *PBL27*, *MKK4*, and *MKK5* were PCR-amplified using gene-specific primers (Appendix Table S1) and ligated into a pENTR/D-TOPO vector (Invitrogen). Point mutations in *MAPKKK5*, *MKK4*, and *MKK5* were generated by PCR-mediated substitution of the sequences encoding the corresponding amino acid residues. A kinase-inactive mutant, *MAPKKK5*^{K375M}, was made by replacing Lys-375 in *MAPKKK5* with Met. The kinase-inactive mutants, *MKK1*^{K97R} and *MKK2*^{K99R}, were made by replacing Lys-97 in *MKK1* and Lys-99 in *MKK2*, respectively, with Arg. The kinase-inactive mutants, *MKK4*^{K108R} and *MKK5*^{K99R}, were made by replacing Lys-108 in *MKK4* and Lys-99 in *MKK5*, respectively, with Arg. *MAPKKK5*^{S617A, S622A, S658A, S660A, T677A, S685A} was made by replacing Ser-617, 622, 658, 660, 685, and Thr-677 in *MAPKKK5* with Ala. *MKK4*^{K108R, T224A, S230A} was made by replacing Thr-224 and Ser-230 in *MKK4* with Ala using a full-length cDNA of *MKK4*^{K108R} as the template. *MKK5*^{K99R, T215A, S221A} was made by replacing Thr-215 and Ser-221 in *MKK5* with Ala using a full-length cDNA of *MKK5*^{K99R} as the template. *MKK2*^{K99R, T229A, S235A} was made by replacing Thr-229 and Ser-235 in *MKK2* with Ala using a

full-length cDNA of *MKK2*^{K99R} as the template. For transient expression in *Nb* leaves, the *MAPKKK5* and *PBL27* coding regions in pENTR/D-TOPO were transferred into the pGWB5 and pGWB14, respectively (Nakagawa *et al*, 2007). For transient expression in *Arabidopsis* protoplasts, the *MAPKKK5* and *PBL27* coding regions in pENTR/D-TOPO were transferred into the p35S-GW-GFP and p35S-GW-3xHA vectors, respectively (Yamaguchi *et al*, 2012).

Chitin-induced immune assay

Arabidopsis seeds were surface-sterilized and germinated in MGRL medium (Naito *et al*, 1994) containing 0.1% agarose and 1% sucrose. Seedlings were grown for 8 days in a 16-h light/8-h dark cycle at 22°C (light) or 20°C (dark). The seedlings were pre-incubated in liquid MGRL medium for 3 h and then treated with 10 μM chitin (GlcNAc)₇. The experiments for MAPK activation and callose deposition were carried out as described previously (Shinya *et al*, 2014). The MAPK activation was determined by immunoblots with anti-phospho-p44/42 MAPK antibody (Cell Signaling #4370).

Pathology assays

Arabidopsis plants were grown in soil for 28–30 days in a growth chamber at 22°C in a 12-h light–dark cycle. Plants were inoculated with 5 μl drops of a spore suspension (7–8 × 10⁵ spores/ml in distilled water) of *Alternaria brassicicola* (isolate O-264) (Narusaka *et al*, 2005). The inoculated plants were placed in a growth chamber at 22°C with a 12-h light–dark cycle and maintained at 100% relative humidity. Lesion sizes were measured at 6 days after inoculation. Control plants were treated with distilled water.

Yeast two-hybrid assays

DNA fragments of *PBL27* and *MAPKKK5* coding regions were transferred into vectors pBTM116 (bait vector) and pVP16 (prey vector). The yeast two-hybrid interaction was analyzed based on the requirement for histidine for yeast growth as described previously (Ishikawa *et al*, 2014). To analyze the protein levels in yeast, yeast cells were resuspended in 100 μl PBS buffer (140 mM NaCl, 2.7 mM KCl, 6.5 mM Na₂HPO₄, 1.5 mM KH₂PO₄ pH 7.4), then 20 μl of SDS sample buffer (350 mM Tris–HCl (pH 6.8), 10% SDS, 3% glycerol, 600 mM DTT, 0.012% bromophenol blue) were added, and incubated at 95°C for 10 min. Proteins were detected by immunoblots with α-VP16 or α-LexA (Santa Cruz Biotechnology sc-7546 or sc-7544) using a ImageQuant LAS4000 (GE Healthcare).

RNA-seq analysis and quantitative RT–PCR

Total RNA was isolated from 8-day-old seedlings harvested at 3 h after treatment with mock or chitin using TRIzol reagent (Invitrogen) and treated with DNase I (Roche). Three independent experiments were performed. RNA libraries were prepared from 1 μg of total RNA using NEBNext Ultra™ Directional RNA Library Prep Kit for Illumina (New England Biolabs) and sequenced on a HiSeq2500 (Illumina) system at the Max Planck-Genome-centre Cologne (<http://mpgc.mpiiz.mpg.de/home/>). Reads were mapped to the *Arabidopsis* genome (tair10) using the splice-aware read aligner TopHat and transformed into a count per gene per library by using

HTSeq (Anders *et al*, 2015). The RNA-seq data used in this study are deposited in the National Center for Biotechnology Information Gene Expression Omnibus database (accession no. GSE74955).

Differentially regulated genes (DRGs; q -value < 0.05) in chitin-treated wild type compared with mock were selected (12,992 genes). DRGs showing reduced induction or suppression (506 genes) or enhanced induction or suppression (151 genes) in *mapkkk5* compared with the wild type (the absolute difference > \log_2 0.5) were selected and shown in the plot as yellow or blue dots, respectively. For the clustering analysis, DRGs that were induced or suppressed more than twofold in wild type compared with mock and that showed reduced induction or suppression in *mapkkk5* compared with wild type (the difference > \log_2 0.5) were selected (339 genes). The heatmap was generated by CLUSTER (Eisen *et al*, 1998) using uncentered Pearson's correlation and complete linkage and visualized by TREEVIEW (Eisen *et al*, 1998).

The statistical analysis of the RNA-seq data was performed in the R environment. Genes with fewer than 120 reads in the sum of all libraries (10 reads per library in average) were discarded. The count data of the remaining genes was normalized with normalization factors calculated by the function `calcNormFactors` in the package `edgeR` and \log_2 -transformed by the function `voom` in the package `limma` to yield \log_2 counts per million. To each gene, a linear model was fit by using the function `lmFit` in the `limma` package with the following terms: $S_{\text{gtr}} = GT_{\text{gt}} + R_r + \epsilon_{\text{gtr}}$, where S , \log_2 expression value, GT , genotype:treatment interaction, and random factors; R , biological replicate; ϵ , residual. The `eBayes` function in the `limma` package was used for variance shrinkage in calculation of the P -values, which was then used to calculate the Storey's q -values using the `qvalue` function in the `qvalue` package.

For the *cis* element enrichment analysis, DRGs that showed reduced induction in *mapkkk5* compared with wild type (the difference > \log_2 0.5) were selected (319 genes). The 1,000 bp upstream of the transcription start sites of the selected genes was tested for enrichment of the known *cis* elements (Franco-Zorrilla *et al*, 2014) against those of the whole *Arabidopsis* genes using AME (McLeay & Bailey, 2010).

Expression levels were quantified by qRT-PCR using SYBR Green master mix (Applied Biosystems) in a Step-One Plus Real-Time PCR system (Applied Biosystems) and normalized against *Actin2* (At2g18780). Three biological replicates were used for each experiment, and two quantitative replicates were performed for each biological replicate.

Transient expression in plant cells

For transient expression in *Nb* leaves, the expression vectors were transformed into *A. tumefaciens*. The transformed *A. tumefaciens* in buffer containing 10 mM MgCl_2 , 10 mM 2-(*N*-morpholine)-ethanesulfonic acid (MES)-NaOH, pH 5.6, and 150 μM acetosyringone was syringe-infiltrated into *Nb* leaves as reported previously (Yamaguchi *et al*, 2012). For transient expression in *Arabidopsis* protoplasts, protoplasts were isolated from 3- to 4-week-old *Arabidopsis* leaves as reported previously (Wu *et al*, 2009). The protoplasts were transfected with the indicated plasmids according to the detail protocol previously described (Yoo *et al*, 2007). The protoplasts were collected 18 h after transfection and subjected to

co-immunoprecipitation and BiFC analyses. The BiFC analyses were carried out as reported previously (Yamaguchi *et al*, 2013; Shinya *et al*, 2014).

Protein analysis

Nb leaves were ground in liquid nitrogen and resuspended in extraction buffer (50 mM Tris-HCl (pH 7.5), 150 mM NaCl, 10% glycerol, 5 mM DTT, 2.5 mM NaF, 1.5 mM Na_3VO_4 , 1 \times complete EDTA-free protease inhibitor cocktail (Roche), and 2% (v/v) IGEPAL CA-630 (MP Biomedicals)). The supernatant was incubated with anti-GFP-Trap beads (Chromotek) or anti-HA magnetic beads (Miltenyi Biotec). The beads were washed four times with the extraction buffer and resuspended in an equal volume of 2 \times SDS sample buffer. Co-immunoprecipitated proteins were analyzed by immunoblots with anti-GFP antibody (Abcam, ab6556) or anti-HA antibody (Sigma, 11-867-423-001). To purify the microsomal fraction, tissue was homogenized on ice with extraction buffer 1 (20 mM Tris-HCl pH 7.5, 0.33 M sucrose, 1 mM EDTA, protease inhibitor cocktail (Roche), 0.1% 2-Me-OH). Crude protein extracts were centrifuged at 2,000 g to remove cell debris, and then the supernatants were centrifuged at 113,500 g for 1 h to pellet microsomal fractions. The supernatants were used as the soluble proteins. Pellets were suspended in extraction buffer 2 [50 mM Tris-HCl (pH 7.5), 150 mM NaCl, 10% glycerol, 5 mM DTT, 2.5 mM NaF, 1.5 mM Na_3VO_4 , 1 \times complete EDTA-free protease inhibitor cocktail (Roche) and 1% (v/v) IGEPAL CA-630 (MP Biomedicals)] and used as the microsomal proteins for this work. α -PIP1 (Cosmo Bio, COP-088) and α -EAP1 (Ishikawa *et al*, 1996) were used as PM and cytosolic markers, respectively.

In vitro kinase activity assays

The recombinant proteins were expressed using a cold-shock bacterial expression system (Takara) and purified using glutathione sepharose 4B (GE Healthcare) and eluted using 50 mM glutathione. The kinase activity assay was performed in 40 μl of reaction mixture containing 50 mM HEPES (pH 7.6), 10 mM MgCl_2 , 100 μM ATP, 1 mM DTT, 1 μg kinase, and 1 μg substrate. The assay was initiated by adding 0.4 μl (4 μCi) [^{32}P] 5-ATP, and the reaction mixture was incubated for 1 h at 25°C. The reaction was terminated by the addition of Laemmli loading buffer and subsequent incubation at room temperature for 10 min. Samples were separated by SDS-polyacrylamide gel electrophoresis. The ^{32}P -labeled bands were detected using an FLA-7000 imaging analyzer (FujiFilm) and Multi Gauge version 3.0 software (FujiFilm).

Identification of phosphorylated amino acid residues

Protein bands were excised from gels stained with Flamingo (Bio-Rad) and subjected to in-gel digestion with trypsin (Fujiwara *et al*, 2014). The digested peptides were loaded on the column (100 μm internal diameter, 15 cm; L-Column, CERI) using a Paradigm MS4 HPLC pump (Michrom BioResources) and an HTC-PAL autosampler (CTC Analytics), and the eluted peptides from the L-column were introduced into a LTQ-Orbitrap XL mass spectrometer (Thermo Scientific, Bremen, Germany). The MS/MS spectra were compared against the TAIR10 database using the MASCOT server. The

MASCOT searches were performed with the following parameters: set off the threshold at 0.05 in the ion-score cutoff, peptide tolerance at 10 ppm, MS/MS tolerance at ± 0.8 Da, peptide charge of 2+ or 3+, one missed cleavage allowed, carbamidomethylation of cysteine as a fixed modification, phosphorylation on serine, threonine, and tyrosine, and oxidation on methionine as a variable modification. The spectrum data of phosphopeptides were confirmed manually.

Expanded View for this article is available online.

Acknowledgements

We thank Prof. Jeff Dangl, HHMI, and UNC Chapel Hill, for critical comments and suggestions for the experiment. We also thank Dr. T. Ueda, Tokyo University, for the detection of GFP fluorescence, S. Sakamoto and N. Mitsuda, AIST, for the *Arabidopsis* protoplast transient assay, Dr. M. Tamoi and Dr. S. Shigeoka for anti-EAP1 antibody, Dr. Y. Kadota for RBOHD construct, and M. Kamei, K. Fukui and R. Funama for technical assistance, and members of the Kawasaki Lab for technical assistance and participation in discussions. This research was supported by Grants-in-Aid for Scientific Research (A) (JP15H02489), for Scientific Research on Innovative Areas (JP15H01242 and JP16H01474), and by the Strategic Project to Support the Formation of Research Bases at Private Universities: Matching Fund Subsidy from the Ministry of Education, Culture, Sports, Science and Technology, 2011–2015 (S1101035) to T.K., Grants-in-Aid for Scientific Research (JP15K18649) and Basic Science Research Projects from Sumitomo Foundation to K. Yamaguchi, Grant-in-Aid for JSPS Fellows to A. Mine, K. Ishikawa and K. Yamada, and the Plant Global Education Project of Nara Institute of Science and Technology to K. Yamada. Tsuda laboratory was supported by the Max Planck Society and by Deutsche Forschungsgemeinschaft (DFG) grant SFB 670.

Author contributions

KYamad, KYamag, and TK designed the project, analyzed the results, and wrote the manuscript. KYamad, KYamag, TS, Kis, YK, and Klc performed experiments. MF, YF, HM, YN, and HN analyzed the phosphorylation sites by mass spectrometry. AM and KT carried out global transcriptional profiling by RNA-seq. MNA and YN analyzed fungal resistance. KS, MNo, YT, TF, and NS provided materials. All authors discussed the results and commented on the manuscript.

Conflict of interest

The authors declare that they have no conflict of interest.

References

Anders S, Pyl PT, Huber W (2015) HTSeq—a Python framework to work with high-throughput sequencing data. *Bioinformatics* 31: 166–169

Ao Y, Li Z, Feng D, Xiong F, Liu J, Li JF, Wang M, Wang J, Liu B, Wang HB (2014) OsCERK1 and OsRLCK176 play important roles in peptidoglycan and chitin signaling in rice innate immunity. *Plant J* 80: 1072–1084

Asai T, Tena G, Plotnikova J, Willmann MR, Chiu WL, Gomez-Gomez L, Boller T, Ausubel FM, Sheen J (2002) MAP kinase signalling cascade in *Arabidopsis* innate immunity. *Nature* 415: 977–983

Bayer M, Nawy T, Giglione C, Galli M, Meinel T, Lukowitz W (2009) Paternal control of embryonic patterning in *Arabidopsis thaliana*. *Science* 323: 1485–1488

Cao Y, Liang Y, Tanaka K, Nguyen CT, Jedrzejczak RP, Joachimiak A, Stacey G (2014) The kinase LYK5 is a major chitin receptor in and forms a chitin-induced complex with related kinase CERK1. *eLife* 3: e03766

Cheng Z, Li JF, Niu Y, Zhang XC, Woody OZ, Xiong Y, Djonovic S, Millet Y, Bush J, McConkey BJ, Sheen J, Ausubel FM (2015) Pathogen-secreted proteases activate a novel plant immune pathway. *Nature* 521: 213–216

Chinchilla D, Zipfel C, Robatzek S, Kemmerling B, Nurnberger T, Jones JD, Felix G, Boller T (2007) A flagellin-induced complex of the receptor FLS2 and BAK1 initiates plant defence. *Nature* 448: 497–500

Clough SJ, Bent AF (1998) Floral dip: a simplified method for *Agrobacterium*-mediated transformation of *Arabidopsis thaliana*. *Plant J* 16: 735–743

Costa LM, Marshall E, Tesfaye M, Silverstein KA, Mori M, Umetsu Y, Otterbach SL, Papareddy R, Dickinson HG, Boutiller K, VandenBosch KA, Ohki S, Gutierrez-Marcos JF (2014) Central cell-derived peptides regulate early embryo patterning in flowering plants. *Science* 344: 168–172

Dangl JL, Horvath DM, Staskawicz BJ (2013) Pivoting the plant immune system from dissection to deployment. *Science* 341: 746–751

Dodds PN, Rathjen JP (2010) Plant immunity: towards an integrated view of plant-pathogen interactions. *Nat Rev Genet* 11: 539–548

Dou D, Zhou JM (2012) Phytopathogen effectors subverting host immunity: different foes, similar battleground. *Cell Host Microbe* 12: 484–495

Eisen MB, Spellman PT, Brown PO, Botstein D (1998) Cluster analysis and display of genome-wide expression patterns. *Proc Natl Acad Sci USA* 95: 14863–14868

Feng F, Yang F, Rong W, Wu X, Zhang J, Chen S, He C, Zhou JM (2012) A *Xanthomonas* uridine 5'-monophosphate transferase inhibits plant immune kinases. *Nature* 485: 114–118

Franco-Zorrilla JM, Lopez-Vidriero I, Carrasco JL, Godoy M, Vera P, Solano R (2014) DNA-binding specificities of plant transcription factors and their potential to define target genes. *Proc Natl Acad Sci USA* 111: 2367–2372

Fujiwara M, Uemura T, Ebine K, Nishimori Y, Ueda T, Nakano A, Sato MH, Fukao Y (2014) Interactomics of Qa-SNARE in *Arabidopsis thaliana*. *Plant Cell Physiol* 55: 781–789

Hayafune M, Berisio R, Marchetti R, Silipo A, Kayama M, Desaki Y, Arima S, Squeglia F, Ruggiero A, Tokuyasu K, Molinaro A, Kaku H, Shibuya N (2014) Chitin-induced activation of immune signaling by the rice receptor CEBiP relies on a unique sandwich-type dimerization. *Proc Natl Acad Sci USA* 111: 404–413

Heese A, Hann DR, Gimenez-Ibanez S, Jones AM, He K, Li J, Schroeder JJ, Peck SC, Rathjen JP (2007) The receptor-like kinase SERK3/BAK1 is a central regulator of innate immunity in plants. *Proc Natl Acad Sci USA* 104: 12217–12222

Huse M, Kuriyan J (2002) The conformational plasticity of protein kinases. *Cell* 109: 275–282

Ichimura K, Shinozaki K, Tena G, Sheen J, Henri Y, Champion A, Kreis M, Zhang SQ, Hirt H, Wilson C, Heberle-Bors E, Ellis BE, Morris PC, Innes RW, Ecker JR, Scheel D, Klessig DF, Machida Y, Mundy J, Ohashi Y et al (2002) Mitogen-activated protein kinase cascades in plants: a new nomenclature. *Trends Plant Sci* 7: 301–308

Ishikawa T, Takeda T, Kohno H, Shigeoka S (1996) Molecular characterization of Euglena ascorbate peroxidase using monoclonal antibody. *Biochim Biophys Acta* 1290: 69–75

Ishikawa K, Yamaguchi K, Sakamoto K, Yoshimura S, Inoue K, Tsuge S, Kojima C, Kawasaki T (2014) Bacterial effector modulation of host E3 ligase activity suppresses PAMP-triggered immunity in rice. *Nat Commun* 5: 5430

Jonak C, Okresz L, Bogre L, Hirt H (2002) Complexity, cross talk and integration of plant MAP kinase signalling. *Curr Opin Plant Biol* 5: 415–424

Jones JD, Dangl JL (2006) The plant immune system. *Nature* 444: 323–329

Kadota Y, Sklenar J, Derbyshire P, Stransfeld L, Asai S, Ntoukakis V, Jones JD, Shirasu K, Menke F, Jones A, Zipfel C (2014) Direct regulation of the NADPH oxidase RBOHD by the PRR-associated kinase BIK1 during plant immunity. *Mol Cell* 54: 43–55

- Kaku H, Nishizawa Y, Ishii-Minami N, Akimoto-Tomiyama C, Dohmae N, Takio K, Minami E, Shibuya N (2006) Plant cells recognize chitin fragments for defense signaling through a plasma membrane receptor. *Proc Natl Acad Sci USA* 103: 11086–11091
- Lee J, Eschen-Lippold L, Lassowskat I, Bottcher C, Scheel D (2015) Cellular reprogramming through mitogen-activated protein kinases. *Front Plant Sci* 6: 940
- Li L, Li M, Yu L, Zhou Z, Liang X, Liu Z, Cai G, Gao L, Zhang X, Wang Y, Chen S, Zhou JM (2014) The FLS2-associated kinase BIK1 directly phosphorylates the NADPH oxidase RbohD to control plant immunity. *Cell Host Microbe* 15: 329–338
- Liu T, Liu Z, Song C, Hu Y, Han Z, She J, Fan F, Wang J, Jin C, Chang J, Zhou JM, Chai J (2012) Chitin-induced dimerization activates a plant immune receptor. *Science* 336: 1160–1164
- Lu D, Wu S, Gao X, Zhang Y, Shan L, He P (2010) A receptor-like cytoplasmic kinase, BIK1, associates with a flagellin receptor complex to initiate plant innate immunity. *Proc Natl Acad Sci USA* 107: 496–501
- Macho AP, Zipfel C (2014) Plant PRRs and the activation of innate immune signaling. *Mol Cell* 54: 263–272
- McLeay RC, Bailey TL (2010) Motif enrichment analysis: a unified framework and an evaluation on ChIP data. *BMC Bioinformatics* 11: 165
- Meng X, Zhang S (2013) MAPK cascades in plant disease resistance signaling. *Annu Rev Phytopathol* 51: 245–266
- Meng X, Chen X, Mang H, Liu C, Yu X, Gao X, Torii KU, He P, Shan L (2015) Differential function of Arabidopsis SERK family receptor-like kinases in stomatal patterning. *Curr Biol* 25: 2361–2372
- Mithoe SC, Ludwig C, Pel MJ, Cucinotta M, Casartelli A, Mbengue M, Sklenar J, Derbyshire P, Robatzek S, Pieterse CM, Aebersold R, Menke FL (2016) Attenuation of pattern recognition receptor signaling is mediated by a MAP kinase kinase kinase. *EMBO Rep* 17: 441–454
- Miya A, Albert P, Shinya T, Desaki Y, Ichimura K, Shirasu K, Narusaka Y, Kawakami N, Kaku H, Shibuya N (2007) CERK1, a LysM receptor kinase, is essential for chitin elicitor signaling in Arabidopsis. *Proc Natl Acad Sci USA* 104: 19613–19618
- Monaghan J, Zipfel C (2012) Plant pattern recognition receptor complexes at the plasma membrane. *Curr Opin Plant Biol* 15: 349–357
- Naito S, Hirai MY, Chino M, Komeda Y (1994) Expression of a Soybean (*Glycine max* [L.] Merr.) seed storage protein gene in transgenic *Arabidopsis thaliana* and its response to nutritional stress and to abscisic acid mutations. *Plant Physiol* 104: 497–503
- Nakagawa T, Kurose T, Hino T, Tanaka K, Kawamukai M, Niwa Y, Toyooka K, Matsuoka K, Jinbo T, Kimura T (2007) Development of series of gateway binary vectors, pGWBs, for realizing efficient construction of fusion genes for plant transformation. *J Biosci Bioeng* 104: 34–41
- Narusaka Y, Narusaka M, Seki M, Ishida J, Shinozaki K, Nan Y, Park P, Shiraishi T, Kobayashi M (2005) Cytological and molecular analyses of non-host resistance of *Arabidopsis thaliana* to *Alternaria alternata*. *Mol Plant Pathol* 6: 615–627
- del Pozo O, Pedley KF, Martin GB (2004) MAPKKKalpha is a positive regulator of cell death associated with both plant immunity and disease. *EMBO J* 23: 3072–3082
- Ranf S, Eschen-Lippold L, Frohlich K, Westphal L, Scheel D, Lee J (2014) Microbe-associated molecular pattern-induced calcium signaling requires the receptor-like cytoplasmic kinases, PBL1 and BIK1. *BMC Plant Biol* 14: 374
- Rasmussen MW, Roux M, Petersen M, Mundy J (2012) MAP kinase cascades in Arabidopsis innate immunity. *Front Plant Sci* 3: 169
- Schwessinger B, Roux M, Kadota Y, Ntoukakis V, Sklenar J, Jones A, Zipfel C (2011) Phosphorylation-dependent differential regulation of plant growth, cell death, and innate immunity by the regulatory receptor-like kinase BAK1. *PLoS Genet* 7: e1002046
- Shi H, Shen Q, Qi Y, Yan H, Nie H, Chen Y, Zhao T, Katagiri F, Tang D (2013) BR-signaling KinaSE1 physically associates with Flagellin Sensing2 and regulates plant innate immunity in Arabidopsis. *Plant Cell* 25: 1143–1157
- Shimizu T, Nakano T, Takamizawa D, Desaki Y, Ishii-Minami N, Nishizawa Y, Minami E, Okada K, Yamane H, Kaku H, Shibuya N (2010) Two LysM receptor molecules, CEBiP and OsCERK1, cooperatively regulate chitin elicitor signaling in rice. *Plant J* 64: 204–214
- Shinya T, Yamaguchi K, Desaki Y, Yamada K, Narisawa T, Kobayashi Y, Maeda K, Suzuki M, Tanimoto T, Takeda J, Nakashima M, Funama R, Narusaka M, Narusaka Y, Kaku H, Kawasaki T, Shibuya N (2014) Selective regulation of the chitin-induced defense response by the Arabidopsis receptor-like cytoplasmic kinase PBL27. *Plant J* 79: 56–66
- Suarez-Rodriguez MC, Adams-Phillips L, Liu Y, Wang H, Su SH, Jester PJ, Zhang S, Bent AF, Krysan PJ (2007) MEKK1 is required for flg22-induced MPK4 activation in Arabidopsis plants. *Plant Physiol* 143: 661–669
- Sun Y, Li L, Macho AP, Han Z, Hu Z, Zipfel C, Zhou JM, Chai J (2013) Structural basis for flg22-induced activation of the Arabidopsis FLS2-BAK1 immune complex. *Science* 342: 624–628
- Tateda C, Zhang Z, Shrestha J, Jelenska J, Chinchilla D, Greenberg JT (2014) Salicylic acid regulates Arabidopsis microbial pattern receptor kinase levels and signaling. *Plant Cell* 26: 4171–4187
- Tsuda K, Mine A, Bethke G, Igarashi D, Botanga CJ, Tsuda Y, Glazebrook J, Sato M, Katagiri F (2013) Dual regulation of gene expression mediated by extended MAPK activation and salicylic acid contributes to robust innate immunity in *Arabidopsis thaliana*. *PLoS Genet* 9: e1004015
- Wu FH, Shen SC, Lee LY, Lee SH, Chan MT, Lin CS (2009) Tape-Arabidopsis sandwich – a simpler Arabidopsis protoplast isolation method. *Plant Methods* 5: 16
- Yamada K, Yamashita-Yamada M, Hirase T, Fujiwara T, Tsuda K, Hiruma K, Saijo Y (2016) Danger peptide receptor signaling in plants ensures basal immunity upon pathogen-induced depletion of BAK1. *EMBO J* 35: 46–61
- Yamaguchi K, Imai K, Akamatsu A, Mihashi M, Hayashi N, Shimamoto K, Kawasaki T (2012) SWAP70 functions as a Rac/Rop guanine nucleotide-exchange factor in rice. *Plant J* 70: 389–397
- Yamaguchi K, Yamada K, Ishikawa K, Yoshimura S, Hayashi N, Uchihashi K, Ishihama N, Kishi-Kaboshi M, Takahashi A, Tsuge S, Ochiai H, Tada Y, Shimamoto K, Yoshioka H, Kawasaki T (2013) A receptor-like cytoplasmic kinase targeted by a plant pathogen effector is directly phosphorylated by the chitin receptor and mediates rice immunity. *Cell Host Microbe* 13: 347–357
- Yoo SD, Cho YH, Sheen J (2007) Arabidopsis mesophyll protoplasts: a versatile cell system for transient gene expression analysis. *Nat Protoc* 2: 1565–1572
- Zhang J, Li W, Xiang T, Liu Z, Laluk K, Ding X, Zou Y, Gao M, Zhang X, Chen S, Mengiste T, Zhang Y, Zhou JM (2010) Receptor-like cytoplasmic kinases integrate signaling from multiple plant immune receptors and are targeted by a *Pseudomonas syringae* effector. *Cell Host Microbe* 7: 290–301
- Zhang Z, Wu Y, Gao M, Zhang J, Kong Q, Liu Y, Ba H, Zhou J, Zhang Y (2012) Disruption of PAMP-induced MAP kinase cascade by a *Pseudomonas syringae* effector activates plant immunity mediated by the NB-LRR protein SUMM2. *Cell Host Microbe* 11: 253–263



License: This is an open access article under the terms of the Creative Commons Attribution-NonCommercial-NoDerivs 4.0 License, which permits use and distribution in any medium, provided the original work is properly cited, the use is non-commercial and no modifications or adaptations are made.